Inflamed Microglia like Macrophages in the Central Nervous System of Prodromal Parkinson's Disease

Le Zhang[1,2,3]*, Yoshiaki Yasumizu[1*,†], M. Elizabeth Deerhake[1]*, Jeonghyeon Moon[1,4], Nicholas Buitrago-Pocasangre[1], Anthony Russo[1,2], Haowei Wang[1,2], Biqing Zhu[5,6], John P. Seibyl[1], Vijaya Reddy[1], Qianchang Wang[7], Maria Grazia Spillantini[3,8], David A. Posner[7], Menna Clatworthy[7], Tomokazu S. Sumida[1,4], Erin E. Longbrake[1], Jesse M. Cedarbaum[1], David A. Hafler*[1,3,4,9,†]

1. Department of Neurology, Yale School of Medicine, New Haven, CT, 06510, USA.
2. Department of Neuroscience, Yale School of Medicine, New Haven, CT, 06510, USA.
3. Aligning Science Across Parkinson's (ASAP) Collaborative Research Network, Chevy Chase, MD 20815, USA.
4. Department of Immunobiology, Yale School of Medicine, New Haven, CT, 06510, USA.
5. Department of Biostatistics, Yale School of Public Health, New Haven, CT, 06510, USA.
6. Program of Computational Biology and Bioinformatics, Yale University, New Haven, CT 06510, USA.
7. Molecular Immunity Unit, University of Cambridge Department of Medicine, Cambridge, UK
8. Department of Clinical Neurosciences, University of Cambridge Department of Medicine, Cambridge, UK
9. Broad Institute of MIT and Harvard, Cambridge, MA, 02142, USA.

* Equally contributed

† Correspondence

Abstract

We investigated the role of inflammation in the pathogenesis of prodromal Parkinson's Disease (PD), performing single-cell RNAseq analysis of cerebrospinal fluid (CSF) and blood from 111 individuals, comparing control subjects with early prodromal PD and later PD to patients with multiple sclerosis (MS). Surprisingly, we identified a pleocytosis in the CSF, most pronounced in patients with early PD. Single-cell RNAseq revealed increases in CSF-specific microglia-like macrophages expressing JAK-STAT and TNFα signaling signatures in prodromal PD, with a lack of T cell activation in the CSF. The CSF macrophages exhibited similar transcriptional profiles to dural macrophages from human α-synuclein-expressing PD model mice. These findings uncover a myeloid-mediated TNFα inflammatory process in the CNS of patients with prodromal PD, suggesting a novel pathological mechanism in disease etiology.

Introduction

Inflammation with activation of both the adaptive and innate immune system is critical in mediating tissue repair [1]. While some degree of inflammation is observed in virtually all central nervous system (CNS) diseases representing responses to tissue injury, primary T cell mediated autoimmunity such as Multiple Sclerosis (MS) can be a primary cause of CNS inflammation. Parkinson's Disease (PD) is a neurodegenerative disorder, predominantly in older populations, characterized by the progressive loss of dopaminergic neurons and the accumulation of α-synuclein aggregates in the brain. Both genetic and pathologic evidence support the notion that CNS inflammation contributes to PD pathogenesis [2-6]. Specifically, the presence of TNFα in microglia and the recent discovery of autoreactive α-synuclein T cells in early PD [7] raises the hypothesis that autoreactive T cells drive early CNS inflammation in prodromal PD, as is seen in relapsing-remitting MS, with later, secondary neurodegeneration manifesting as classic PD [8-13].

We recently identified myeloid cells in the cerebrospinal fluid (CSF) expressing microglia-associated cell surface proteins, such as APOE, C1Q, and TREM2, that are presumably derived from a monocyte lineage. While first observed in higher numbers in the CSF of patients with HIV[14], they are also observed in the CSF of healthy subjects. These CSF microglia-like macrophages share gene expression patterns with border-associated macrophages located along the brain vasculature at the interface of the brain parenchyma [15,16]. Surprisingly, the frequency of this population of microglia-like macrophages was markedly decreased in the CSF of patients with autoimmune, relapsing-remitting MS as compared to age-matched healthy controls [17]. With highly effective B cell depletion therapy, this population re-emerged in the CSF of MS patients, with associated increases in myeloid TNFα expression in both CSF and blood, suggesting an important role in autoimmune disease pathogenesis [17].

One early clinical manifestation of α-synucleinopathy is Rapid Eye Movement Sleep Behavior Disorder (RBD), a parasomnia that can appear years or even decades before the onset of typical symptoms of PD or Dementia with Lewy Bodies (DLB) [18]. Thus, RBD serves as an early indicator of future α-synuclein-related neurodegeneration. Additionally, there is strong epidemiologic data indicating a link between autoimmune disorders, such as inflammatory bowel disease and PD, adding further support for a prominent role for the immune system in mediating the inception and progression PD pathology [19,20]. Thus, examining whether there is CNS inflammation in RBD as a manifestation of prodromal synucleinopathy and determining the pathways mediating inflammation can provide a rationale for clinical experiments to prevent the

disease and to provide more convincing evidence that an early autoimmune process proceeds a secondary neurodegenerative form of disease.

Here, we performed single-cell RNAseq analysis of CSF and blood from 84 individuals, including 34 with RBD, 18 with PD without RBD, 15 PD and RBD, 15 age-matched healthy controls, and 29 patients with recent onset MS. We unexpectedly identified a lymphocytic pleocytosis in the CSF of patients with RBD, that was not present in patients with longer standing PD, similar to what is observed in patients with autoimmune MS. However, in marked contrast to MS, single-cell RNAseq in prodromal PD revealed an increase in the frequency and cell numbers of CSF microglia-like macrophages expressing IL6-JAK-STAT3 and TNFα signaling pathways. This inflammatory signature was shared with that of brain microglia of PD patients and CNS-dural sinus myeloid cells and border-associated macrophages in PD model mice expressing human truncated α-synuclein in dopaminergic neurons. These findings reveal a myeloid-mediated TNFα inflammatory process in the CNS during the prodromal stage of PD, suggesting a newly described pathologic process in disease etiology.

Results

Single-cell immune atlas of PBMCs and CSF in prodromal and early stage of PD

To profile the immunological changes in prodromal and across PD stages, we generated a single-cell RNAseq immune atlas from paired peripheral blood mononuclear cells (PBMCs) and CSF cells. A total of 84 participants were enrolled, of whom 73 contributed blood and CSF samples suitable for analysis and categorized into four groups: RBD (n=36), PD without RBD (described as PD; n=15), PD with RBD (described as PD-RBD; n=18), and age-matched healthy controls (HC; n=15) (Table S1,2). Clinical and demographic information was collected, and PBMCs and CSF samples were obtained from all participants. The demographic and clinical characteristics of our study population were similar to other cohorts (Table S1). The mean ages of the subjects in the four groups ranged from 64 to 89 years; 77% were males. Of the RBD group, 19 (53%) were hyposmic, as defined by an UPSIT score below the 15th percentile for age and gender [21], 7 (19%) evidenced reduced dopamine transporter (DaT) binding in the striatum, and 25 (69%) showed Synuclein Aggregating Activity (SAA) in their CSF. In all, 26 (72%) of the RBD subjects met MDS Prodromal PD Likelihood Ratio criteria for prodromal PD [22], and were thus defined as a “high-risk” population. Of the subjects who entered with a diagnosis of RBD, six were diagnosed with either PD or Lewy Body Dementia (LBD) during the course of the study.

We first examined the CSF for evidence of inflammation by quantitative analysis of approximately ~30 mL of CSF from each subject. Unexpectedly, subjects with RBD showed an

increase of CSF cells compared to age-matched HC subjects (3.3 + 2.3 vs 1.4 $\pm$ 0.7 cells/uL; p = 0.045, ANOVA followed by Tukey-Kramer post-hoc test; Fig. 1A), indicative of inflammation in the CNS of prodromal PD patients. We then performed droplet-based single-cell RNAseq with VDJ sequencing using the 10x Genomics Chromium platform. After stringent quality control, 523,521 cells from PBMCs (73 donors) and 259,560 cells from CSF (72 donors) were retained (Fig. 1B-F, Fig. S1A). The average number of genes and percentage of mitochondrial genes detected per cell across all samples were 1,833 genes and 2.67% in PBMCs and 1,929 genes and 1.83% in CSF, respectively, reflecting high-quality single-cell transcriptomic data across both sample types. Based on the clusters defined by unsupervised clustering, we identified major immune cell types: B cells, myeloid cells, T cells, and NK cells in both PBMCs and CSF. Subclusters within these groups were further annotated based on known marker genes, resulting in 24 clusters in PBMCs and 20 clusters in CSF (Fig. 1D-G, Fig. S1B,C). The cell cluster annotations were validated using CellTypist [23] (Fig. S2E,F).

In PBMCs, the proportions of immune cells were as follows: B cells 8.09%, myeloid cells 20.8%, T cells 59.6%, and NK cells 11.0% (Fig. 1D). In contrast, CSF showed distinctly different proportions consistent with our previous findings [24]: B cells 0.53%, myeloid cells 23.8%, T cells 73.0%, and NK cells 2.59% (Fig. 1F). Compared to PBMCs, CSF had a higher proportion of T cells and myeloid cells, and a lower proportion of B cells and NK cells. At the subcluster level, specific differences were observed. For example, populations such as CD4 T naive cells (15.9% in PBMC, 5.62% in CSF), $CD16^+$ monocytes (3.56% in PBMC, 0.09% in CSF), and $CD16^+$ NK cells (10.0% in PBMC, 0.34% in CSF) were less abundant in CSF, while clusters such as cDC2 (1.06% in PBMC, 3.98% in CSF) and CD4 T central memory (Tcm) cells (12.3% in PBMC, 41.6% in CSF) were enriched. As we previously reported[14], microglia-like macrophages in the CSF (termed CSF Mac), which expressed *C1QC* and *TREM2* specifically, were the most abundant myeloid cell population in CSF and were uniquely observed in this compartment. These findings suggest that, while the CSF immune environment largely consists of circulating immune cells similar to those in PBMCs, it exhibits significant differences in cell composition. The CSF likely represents a unique immune microenvironment linked to the CNS and CNS borders. Overall, we successfully constructed a single-cell immune cell atlas of PBMCs and CSF in RBD and PD.

Pronounced immunological changes in prodromal PD

To identify PD-specific immune alterations, we analyzed our single-cell immune atlas to assess both quantitative changes (shifts in cell frequencies and absolute cell numbers) and qualitative changes (alterations in gene expression). To evaluate changes in cell frequencies,

we used a Bayesian model [25] to compare RBD, PD, and PD-RBD groups against age-matched healthy controls (Fig. 2A-C). RBD exhibits heterogeneity in features such as hyposmia and CSF SAA status, both of which are known to be associated with PD onset [26]. Using these factors, we further stratified RBD individuals based on predicted PD risk [22]. This analysis revealed a significant increase in the CSF Mac population in the RBD high-risk group (Fig. 2B,C). Additionally, the absolute numbers of CSF Mac, $CD4^+$ Tnaive, Tcm, and Tem cells in CSF were increased as compared to healthy controls (Fig. 2D) while there was a decrease in the relative proportion of $CD4^+$ Tcm cells and $CD8^+$ T effector memory/terminally differentiated effector memory (em/emra) cells in the RBD group (FDR < 0.05 and < 0.1 respectively). As previously described [27], we observed an increase in $CD4^+$ T naive cells in the peripheral blood of prodromal PD (FDR < 0.05).

We next examined gene expression changes within each cluster (Fig. S2A). Compared to PBMCs, we observed more pronounced gene expression changes in CSF, especially in $CD4^+$ T cells, $CD14^+$ monocytes, and the CSF Mac population. Notably, when stratifying RBD patients by MDS Prodromal PD probability score, the RBD high-probability group exhibited the highest number of differentially expressed genes (DEGs). These findings suggest that both cell frequency and gene expression changes are most pronounced in the RBD high-probability group, with relatively smaller differences observed in PD and PD-RBD. Furthermore, in CSF, $CD4^+$ T cells and CSF Mac demonstrated coordinated changes in both cell numbers and gene expression.

To interpret these gene expression changes, we calculated scores for each cell population across conditions using Hallmark gene sets from the Molecular Signatures Database (MSigDB) (Fig. 2E, S2B-F, Table S3,4). In PBMCs, oxidative phosphorylation was broadly upregulated in T cells from RBD and PD-RBD patients, suggesting that peripheral circulating T cells maintain a homeostatic state, consistent with the observed increase in naive $CD4^+$ T cells. In CSF, the most pronounced gene program changes were detected in myeloid populations, particularly in CSF Mac. In the RBD group, significant enrichment of pathways such as mitotic spindle (Mean change = 0.640, padj=4.33×10^{-302}), inflammatory response (Mean change = 0.689, padj=2.45×10^{-189}), IL6-JAK-STAT3 signaling (Mean change = 0.447, padj=3.97×10^{-166}), and TNFα signaling via NF-κB (Mean change = 0.807, padj=2.84×10^{-96}), were observed. These findings suggest heightened cellular activity and immune responses in the CSF Mac population in prodromal PD.

Inflammatory signature in MS versus RBD CSF

A major paradox in the field of autoimmunity revolves around the TNFα pathway, presumably relating to the different genetic architectures of human autoimmune diseases [28,29]. Specifically, while anti-TNFα therapy is an effective treatment for Inflammatory Bowel Disease (IBD) and rheumatoid arthritis (RA), it paradoxically induces exacerbations in patients with MS[30,31]. Moreover, three independent studies have shown a highly significant decrease in the incidence of PD in IBD patients on anti-TNFα therapy with an increased concordance of IBD and PD [19,20]. Based on these observations, we hypothesized that the CSF Mac population in prodromal PD would be characterized by elevated TNFα signaling and exhibit a distinct gene expression profile compared to MS. We analyzed single-cell dataset of CSF cells from 29 MS patients and 7 age-matched healthy individuals. As recently reported in a different MS dataset [17], we observed a marked reduction in the CSF Mac population that was confirmed with a recent meta-analysis of other MS datasets (Fig. 3C) [16,17,32]. Gene set enrichment analysis revealed a pattern opposite to that observed in RBD, with strong enrichment of gene sets in T cells, B cells, and dendritic cells, while enrichment in CSF macrophages was minimal (Fig. 3E, Table S5). Notably, TNFα signaling via NF-κB showed a negative change in MS CSF Mac (Mean change=-0.716, padj=4.75×10^{-5}). Furthermore, we applied (1) a detailed analysis pipeline specialized for circulating $CD4^+$ T cells [33,34] and (2) TCR-based estimation of T cell activity [35]. Both approaches consistently suggested that T cells are not activated in PD or RBD (Supplementary Note). These findings suggest that the regulatory mechanisms governing CSF Mac population differ between MS and PD, particularly in the context of TNFα signaling pathway.

Inflammatory signature in CSF Macrophages

We conducted a detailed analysis of CSF Mac, which exhibited notable quantitative and qualitative changes. As previously described, CSF Mac population shares transcriptomic similarity with microglia and expresses macrophage markers, such as *C1QC*, *APOE*, and *TREM2,* at higher levels compared to other myeloid populations (Fig. 3A-C) [14,16,17]. Previous studies also suggested this population resembles border-associated macrophages [15,16]. To further analyze the tissue specificity of this CSF Mac population and its similarity with microglia, we integrated myeloid populations from both PBMCs and CSF with publicly available datasets of microglia [36] and cross-tissue myeloid cells [23], comparing their expression profiles (Fig. S3). While the analysis as expected revealed that CSF Mac population was transcriptionally close to microglia and tissue-resident macrophages, distinct differences were also observed. For instance, *SPP1*, *P2RY12*, and *TMEM119* were more highly expressed in microglia than in CSF Mac (Fig. S3). These findings highlight both the similarities and the divergence in expression patterns between CSF Mac and microglia. We next compared the gene expression of CSF Mac between controls and RBD. The analysis revealed upregulation of HLA class II molecules and

their regulator *CIITA*, as well as increased expression of *HIF1A*, mitochondrial genes, AP1 family genes, *JAK2*, *TLR2*, and *TNFRSF1A* and *TNFRSF1B* in RBD (Fig. 3D,E, Table S6). These changes were consistent with hallmark gene set analyses, which showed elevated scores for pathways such as inflammatory response and IL6-JAK-STAT3 signaling in RBD patients (Fig. 3F). Both RNA seq and flow cytometry analysis revealed an increase in integrin alpha 4 subunit (ITGA4), a key molecule for CNS homing, in $CD16^+$ monocytes from the blood of RBD low-risk individuals, suggesting that monocyte migration to the CNS is more active during the prodromal phase of PD (Fig. 3G). This finding suggests that the activation of myeloid cells in peripheral blood is reflected later than in the CSF.

We further hypothesized that CSF Mac might be functionally linked to microglial changes occurring in the brains of PD patients. To test this hypothesis, we utilized publicly available single-nucleus RNAseq data profiling multiple brain regions from 100 donors, including 75 PD cases [37]. The analysis revealed that genes upregulated in CSF Mac in RBD were also significantly upregulated in the primary motor cortex and prefrontal cortex of PD brains (Fig. S4A,B). These results suggest that CSF Mac are not only activated during the prodromal phase of PD but also reflect microglial changes occurring within the PD brain. In addition, we attempted to examine myeloid populations in the CNS border region. As dural tissue was not available, we examined dural myeloid cells from PD model mice expressing aggregation-prone truncated human α-synuclein under the control of the tyrosine hydroxylase promoter [38] (material and methods). The dural macrophage expressed CSF Mac marker genes such as *Trem2*, *Apoe*, and *C1qc* (Fig. S4C). We found that TNFα related genes and MHC class II genes were upregulated in PD model mice, consistent with the changes observed in CSF Mac in prodromal PD. These data suggest that synchronized gene expression changes occur in brain parenchymal microglia, CNS-broader macrophage, and CSF Mac in prodromal and clinical stages of PD.

Enhanced cell-cell communication in the immune landscape of RBD

Next, we examined cell-cell interactions in the CSF using CellPhoneDB[39]. The ligand—receptor interaction prediction suggested that myeloid cells, including CSF Mac and cDC2, would exhibit robust ligand—receptor signals and that there would be more interactions between lymphocytes and myeloid cells than among lymphocytes alone (Fig. 4A). Focusing on the RBD group, which observed more pronounced immunological changes, we investigated cell-cell interaction pairs with substantial shifts in signaling dynamics. We found that ligands associated with signaling were moderately elevated (FDR<0.2) in lymphocyte subsets such as CD4 Tcm, NK CD16, and memory B cells, whereas receptor signals were enhanced (FDR<0.2)

in myeloid subsets including cDC2 and CSF Mac (Fig. 4B). Notably, the strongest elevation in receptor mediated signals occurred among myeloid cells themselves, suggesting the presence of autonomous feedback activation. To explore these analyses further, we examined autonomous ligand—receptor pairs in CSF Mac and identified several upregulated pairs in RBD, including *C3–C3AR1*, *CD55–ADGRE5*, and *LGALS9–HAVCR2* (Tim3), which are associated with immunoregulatory functions (Fig. 4C). Additionally, we detected neurodegeneration-related signals mediated by amyloid precursor protein (*APP–CD74*, *APP–SORL1*) and prion protein (*PRNP–ADGRG6*). It is also known that aggregated α-synuclein can induce the activation of myeloid cells [40]. These ligand—receptor pairs may modulate the activation state of CSF macrophages and influence the CNS microenvironment. In particular, CSF Mac may help process and clear disease-associated proteins such as α-synuclein, while simultaneously suppressing excessive inflammation via Tim3 and complement regulation as reported in microglia [41] (Fig. 4D). Collectively, these dynamic and comprehensive changes in cell-cell interactions appear to play a critical role in shaping the immune landscape during the prodromal stage of PD.

Genetic prioritization of cell populations highlighted myeloid population in CSF

To determine whether integrating known genetic information with our immune cell atlas could aid in prioritizing relevant cell populations in PD, we analyzed both polygenic and rare variant components. First, we used scDRS [42] to integrate GWAS data associated with PD [4], RBD [43], and LBD [44] traits, evaluating the enrichment of polygenic signals in individual cell types (Fig. S5A,B). The analysis revealed the strongest polygenic signal in CSF Mac for LBD. Note that LBD [44] shares genetic risks with both PD and Alzheimer's disease, suggesting it may not be a pure synucleinopathy. For PD, significant associations were observed in cDC2 and pDC in blood and pDC in CSF. No significant associations were detected for RBD, although polygenic signals appeared to accumulate in myeloid populations within the CSF.

We further examined the expression of PARK genes, which have been identified as causative variants in familial PD, within the CSF (Fig. S6). Although some genes, such as *PARK7* and *CHCHD2*, displayed ubiquitous expression, the overall trend indicated higher expression within myeloid cells. When focusing on CSF Mac, we observed that multiple genes, including *SNCA* (encoding α-synuclein), *PRKN*, *LRRK2*, *PINK1*, and *VPS35* were upregulated in RBD and PD. In contrast, *PARK7* and *CHCHD2* showed higher expression in controls, with reduced levels in RBD and PD, suggesting a loss-of-function role of these genes in PD. Together, these results suggest that, beyond polygenic signals, familial Parkinson's disease variants also converge in CSF myeloid cell populations, especially in CSF Mac.

Discussion

While emerging evidence suggests an underlying inflammatory etiology for PD as demonstrated by the presence of α-synuclein autoreactive T cells in the circulation of a proportion of patients with manifest and prodromal PD, pathological studies reveal only a minimal presence of $CD8^+$ T cells in the substantia nigra of PD patients early in disease pathogenesis [45]. To elucidate early mechanisms of disease pathogenesis in PD, we performed single-cell RNAseq analysis of paired CSF and blood from 84 subjects with different stages of PD and compared them to 15 age-matched healthy subjects and 29 patients with MS. We found a previously unrecognized pleocytosis that is most pronounced in patients with RBD, a prodromal synucleinopathy. In prodromal PD CSF, single-cell RNAseq analysis revealed increased frequencies of a population of microglia like macrophages, termed CSF Mac, exhibiting inflammatory responses characterized by increased expression of IL6-JAK-STAT3 and *TNFRSF1A* and *TNFRSF1B* signaling pathways, with a prominent lack of T cell activation. This is the opposite of what is observed in MS CSF where these is a loss of CSF Mac and increases in activated T cells. Single cell analysis of peripheral blood monocytes in in early prodromal PD revealed increased expression of ITGA4 in circulating CD16 monocytes that was confirmed by flow cytometry consistent with monocyte migration into the CNS. Thus, these findings reveal a myeloid mediated inflammatory process in the CNS of patients with prodromal PD, suggesting a novel pathologic mechanism in disease etiology of PD.

We compared immune populations with single-cell resolution in the CSF of subjects with new-onset MS and RBD. In contrast to MS CSF, where we observed a decreased frequency of CSF Mac, this macrophage population expressing microglia-like features was increased in the CSF of patients with prodromal PD, with a pronounced TNF/IL-6/JAK-STAT signature. Inhibition of the JAK/STAT pathway has been implicated in exerting protective effects in PD [46-48]. In addition, treatment of MS with B cell depletion is 98% effective in preventing new inflammatory exacerbations; concurrently, the CSF Mac population becomes exponentially expanded in the CSF with increased secretion of TNFα by circulating monocytes [17]. Taken together, these data suggest fundamental differences in the activity of TNFα pathways between prodromal PD and MS. Moreover, these experimental results are consistent with large-scale epidemiologic investigations of patients with IBD, demonstrating that anti-TNFα can substantially decrease the incidence of new-onset PD [19].

Our observations comparing PD and MS are in line with a fundamental observation of human inflammatory diseases. Specifically, the therapeutic efficacy found with blocking an inflammatory pathway in one autoimmune disease can lead to flare-ups in other autoimmune

diseases. Two prominent examples include anti-IL-17 blockade that has strong efficacy in treating psoriasis but has the risk of new onset or exacerbation of IBD [49]. Another example is anti-TNFα blockade, an effective treatment in IBD and rheumatoid arthritis that can cause exacerbations in patients with MS [31]. These paradoxical observations are related to the different genetic architectures of autoimmune diseases where a risk haplotype in one disease can be protective in another [28]. Thus, we hypothesized that comparing the TNFα pathways among different CNS inflammatory diseases may give insight into disease pathogenesis. However, only a randomized control investigation of patients with prodromal PD can provide definitive evidence for a role of TNFα in the pathogenesis of PD.

Compared to the significant changes in the CSF myeloid populations, relatively minor changes in T cell populations were observed in prodromal PD. Specifically, our analysis replicated previous studies [27] showing increases in circulating and CSF naïve $CD4^+$ cells in prodromal PD and PD with reductions in the proportion of $CD4^+$ Tcm cells and $CD8^+$ Temra cells in CSF. Additionally, recent studies by Sulzer and co-workers demonstrated that activated α-synuclein reactive T cells in mouse models of PD cause inflammation in the gut tissue with the absence of CNS inflammation. These results are in contrast to T and B cell populations in patients with early relapsing/remitting MS, which display markedly inflammatory signals in CSF T cells and in parenchymal lesions which are relatively absent in prodromal PD. The prominent activation of CSF myeloid cells in the absence of T cell activation in prodromal PD suggest a fundamentally different mechanism of autonomous neuroinflammation mediated predominantly by the innate as opposed to the adaptive immune system. In this regard, synchronized myeloid cell activations in brain parenchymal microglia, CNS-broader macrophage are observed that are in equilibrium with human CSF Mac.

In summary, these observations in mouse models and direct examination of humans with prodromal PD leads us to hypothesize that the disease begins with activation of α-synuclein reactive T cells in the gut, perhaps related to the known microbiome dysbiosis in PD patients, leading to aggregation of α-synuclein in the intestines. It is known that α-synuclein can propagate from the gut, via the vagus nerve, to the brain [50], where it has been shown that α-synuclein aggregates can activate CNS border-associated macrophages [40] and dural myeloid cells, which are synchronized with the CSF Mac. In this model, α-synuclein–reactive T cells may act locally in the dura sinuses as suggested by mouse model and not directly in the brain parenchyma, consistent with our observations in human that in total contribute to the degeneration of CNS dopamine-producing neurons. Together, these data suggest a novel mechanism of myeloid cells as opposed to T cell-mediated autoimmune disease.

Figure Legends

Figure 1: Single-cell immune atlas of PBMCs and CSF in prodromal and early stage of PD.

(A) CSF cell counts. (HC: 1.4 $\pm$ 0.7; RBD: 3.3 + 2.3, PD: ?? cells/uL; p = 0.045, ANOVA followed by Tukey-Kramer post-hoc test) (B) Schematic overview of the project workflow. (C-F) Uniform Manifold Approximation and Projection (UMAP) plots of single-cell data (C,E) and corresponding cell frequencies (D,F) for blood (C,D) and CSF (E,F). Error bars indicate 95% confidence intervals (D,F).

Figure 2: Global characterization highlighted activation of CSF Macrophages in prodromal PD.

(A,B) Cell population changes for RBD, PD, and PD-RBD were analyzed in Blood (A) and CSF (B) using scCODA [25] (a Bayesian statistical tool) relative to HC, with RBD stratified by PD risk score (right heatmaps). See materials and methods for the details. FDR thresholds: 0.05, '**'; 0.1, '*'. Color indicates fold change in relative cell frequency. The RBD high-risk group is outlined with dotted lines. (C) CSF macrophages exhibited significant alterations, shown by per-patient frequencies (right). The frequencies in MS [17] and age-matched HC are also shown (left). For PD cohort, the scCODA statistical significance is marked similarly with (A,B). For MS, Statistical testing was performed using the Mann–Whitney U test for each cell population, followed by multiple testing corrections. The adjusted p-value was 1.12×10^{-4}. (D) The absolute cell number of CSF Mac was and T cell populations calculated by the proportion of the cell from scRNAseq and the cell count data. (E) Hallmark gene sets enriched in MS (upper) and RBD (lower) across cell types in comparison to HC (materials and methods). Only positively associated gene sets were visualized. The dashed line at the bottom indicates Padj = 0.05. See Fig. S2 for other comparisons. Only positively associated gene sets were visualized. The dashed line at the bottom indicates Padj = 0.05. (A,B,E lower) Panels include only clusters containing >1000 cells for blood and >500 cells for CSF. (E upper) The same cell types with (F) were retained for the visualization.

Figure 3: CSF macrophages activation and linked gene patterns with PD brain microglia.

(A) Myeloid cell populations in CSF on UMAP embeddings. (B) Dot plot depicting signature genes' mean expression levels and percentage of cells expressing them across clusters. Marker genes for the plot were manually selected. (C) Heatmap showing the transcriptome correlation between myeloid cell populations. (D) Volcano plot showing the differential expressed genes in CSF Macrophage (CSF Mac) between RBD vs HC. For the visualization, genes with mean expression > 0.5 were selected. Genes with FDR < 0.1, Log2 fold change > 0.2 or < -0.2 were highlighted in red. (E) Heatmap showing scaled mean expression of the representative genes. The value was scaled for each gene. (F) Sample-wise HALLMARK gene set activity. *: FDR < 0.05. (G) Mean Fluorescence Intensity (MFI) distribution of IGTA4 in $CD16^{+}$ Monocytes. (p=0.0147)

Figure 4: Cell-cell interaction analysis showed enhanced receiver activity in CSF myeloid cell populations

(A) The heatmap showing the number of interactions inferred by CellphoneDB [39]. The x-axis shows the sender, and the y-axis shows the receiver. (B) The activated ligand-receptor pairs in RBD compared to HC (materials and methods). The upregulated sender signals (upper) and receiver signals (lower) are shown. Interactions with FDR < 0.2 are shown in the black lines. Potentially upregulated interactions (p < 0.05) were shown in the dashed grey lines. (C) Heatmaps show fold change in disease conditions compared to HC for representative CSF Mac ligand-receptor pairs. (D) Dot plot showing the expression of HAVCR2 across CSF myeloid cell populations (upper) and in CSF Mac population across conditions (lower).

Acknowledgement

We also acknowledge Yale Center for Genome Analysis for 10x Genomics library preparation and Illumina sequencing and Dr. Brian Koo for assistance in patient collections. The illustrations were generated using BioRender.com.

Funding

This work was supported by Aligning Science Across Parkinson's (ASAP: D.A.H., L.Z., and M.G.S.). D.A.H also receives research support from Hoffmann-La Roche Pharmaceuticals and Genentech. The study is funded by the joint efforts of the Michael J. Fox Foundation for

Parkinson's Research (MJFF) and the ASAP initiative. MJFF administers the grant (ASAP-000529) on behalf of ASAP and itself. L.Z. is supported by NIH grants (DP2 DA056169, R56 AG074015). Y.Y. is supported by JSPS Overseas Research Fellowships. D.A.H. is supported by NIH grants (P01 AI073748, U19 AI089992 U24 AI11867, R01 AI22220, UM 1HG009390, P01 AI039671, P50 CA121974, R01 CA227473), Race to Erase MS and National MS Society. D.A.H. and J.M.C. are supported by a grant from the Marcus Foundation (Grant # AWD0011411)

COI

D.A.H. has received research funding from Bristol-Myers Squibb, Sanofi, Genentech, and Hoffman LaRoche. He has been a consultant for Repertoire Inc, Bristol Myers Squibb, Genentech, Novartis Pharmaceuticals, and Sanofi Genzyme. J.M.C has received consulting fees from VanquaBioa, Inc.

Author Contributions

L.Z., Y.Y., M.E.D., J.M.C., and D.A.H. conceptualized the study. L.Z., J.M., A.R., and H.W. performed the experiments. Y.Y., M.E.D., B.Z., L.Z., J.P.S, and V.R. analyzed the data. Q.W., M.G.S., D.A.P., and M.C. generated mouse scRNAseq data. Y.Y., L.Z., J.M.C., and D.A.H. wrote the manuscript. A.R., H.W., V.R., N.P., E.E.L., J.M.C., and D.A.H. collected clinical samples. Y.Y., L.Z., J.M.C., T.S.S., and D.A.H. supervised the project.

Data and Materials Availability

Codes will be available on Github (https://github.com/yyoshiaki/2025_PD_PBMCCSF_scRNAseq) upon acceptance. Raw fastq files Raw fastq files will be available in the ASAP CRN cloud for the PD and RBD cohort, and dbGAP and GEO for the MS cohort upon acceptance. The processed scRNA-seq data will be available in CZ CELLxGENE upon acceptance.

Reference

1 Kim, M. W. *et al.* Endogenous self-peptides guard immune privilege of the central nervous system. *Nature* **637**, 176-183 (2025). https://doi.org/10.1038/s41586-024-08279-y

2 Jo, M. G., Kim, S. H. & Yun, S. P. Hidden face of Parkinson's disease: is it a new autoimmune disease? *Neural Regen Res* (2024). https://doi.org/10.4103/NRR.NRR-D-24-01063

3 Kim, J. J. *et al.* Multi-ancestry genome-wide association meta-analysis of Parkinson's disease. *Nat Genet* **56**, 27-36 (2024). https://doi.org/10.1038/s41588-023-01584-8

4 Nalls, M. A. *et al.* Identification of novel risk loci, causal insights, and heritable risk for Parkinson's disease: a meta-analysis of genome-wide association studies. *Lancet Neurol* **18**, 1091-1102 (2019). https://doi.org/10.1016/S1474-4422(19)30320-5

5 Qu, Y. *et al.* A systematic review and meta-analysis of inflammatory biomarkers in Parkinson's disease. *NPJ Parkinsons Dis* **9**, 18 (2023). https://doi.org/10.1038/s41531-023-00449-5

6 Yu, E. *et al.* Fine mapping of the HLA locus in Parkinson's disease in Europeans. *NPJ Parkinsons Dis* **7**, 84 (2021). https://doi.org/10.1038/s41531-021-00231-5

7 Lindestam Arlehamn, C. S. *et al.* alpha-Synuclein-specific T cell reactivity is associated with preclinical and early Parkinson's disease. *Nat Commun* **11**, 1875 (2020). https://doi.org/10.1038/s41467-020-15626-w

8 Sommer, A. *et al.* Th17 Lymphocytes Induce Neuronal Cell Death in a Human iPSC-Based Model of Parkinson's Disease. *Cell Stem Cell* **24**, 1006 (2019). https://doi.org/10.1016/j.stem.2019.04.019

9 Sulzer, D. *et al.* T cells from patients with Parkinson's disease recognize alpha-synuclein peptides. *Nature* **546**, 656-661 (2017). https://doi.org/10.1038/nature22815

10 de Fabregues, O. *et al.* Relevance of tissue-resident memory CD8 T cells in the onset of Parkinson's disease and examination of its possible etiologies: infectious or autoimmune? *Neurobiol Dis* **187**, 106308 (2023). https://doi.org/10.1016/j.nbd.2023.106308

11 Furusawa-Nishii, E. *et al.* alpha-Synuclein orchestrates Th17 responses as antigen and adjuvant in Parkinson's disease. *J Neuroinflammation* **22**, 38 (2025). https://doi.org/10.1186/s12974-025-03359-w

12 Jiang, Z. *et al.* The role of the immune system in Parkinson's disease pathogenesis: A focus on Th17 cells - A systematic review and meta-analysis. *J Neuroimmunol* **398**, 578484 (2025). https://doi.org/10.1016/j.jneuroim.2024.578484

13 Bolte, A. C. & Lukens, J. R. Th17 Cells in Parkinson's Disease: The Bane of the Midbrain. *Cell Stem Cell* **23**, 5-6 (2018). https://doi.org/10.1016/j.stem.2018.06.016

14 Farhadian, S. F. *et al.* Single-cell RNA sequencing reveals microglia-like cells in cerebrospinal fluid during virologically suppressed HIV. *JCI Insight* **3** (2018). https://doi.org/10.1172/jci.insight.121718

15 Ostkamp, P. *et al.* A single-cell analysis framework allows for characterization of CSF leukocytes and their tissue of origin in multiple sclerosis. *Sci Transl Med* **14**, eadc9778 (2022). https://doi.org/10.1126/scitranslmed.adc9778

16 Cantoni, C. *et al.* A single-cell compendium of human cerebrospinal fluid identifies disease-associated immune cell populations. *J Clin Invest* **135** (2025). https://doi.org/10.1172/JCI177793

17 Wei, J. *et al.* Transcriptomic profiling after B-cell depletion reveals central and peripheral immune cell changes in multiple sclerosis. *J Clin Invest* (2025). https://doi.org/10.1172/JCI182790

18 Postuma, R. B., Gagnon, J. F., Bertrand, J. A., Genier Marchand, D. & Montplaisir, J. Y. Parkinson risk in idiopathic REM sleep behavior disorder: preparing for neuroprotective trials. *Neurology* **84**, 1104-1113 (2015). https://doi.org/10.1212/WNL.0000000000001364

19 Peter, I. *et al.* Anti-Tumor Necrosis Factor Therapy and Incidence of Parkinson Disease Among Patients With Inflammatory Bowel Disease. *JAMA Neurol* **75**, 939-946 (2018). https://doi.org/10.1001/jamaneurol.2018.0605

20 Potashman, M. *et al.* The impact of anti-inflammatory therapy on Parkinson's disease incidence: A retrospective cohort study. *Parkinsonism Relat Disord* **130**, 107194 (2025). https://doi.org/10.1016/j.parkreldis.2024.107194

21 Brumm, M. C. *et al.* Updated Percentiles for the University of Pennsylvania Smell Identification Test in Adults 50 Years of Age and Older. *Neurology* **100**, e1691-e1701 (2023). https://doi.org/10.1212/WNL.0000000000207077

22 Berg, D. *et al.* MDS research criteria for prodromal Parkinson's disease. *Mov Disord* **30**, 1600-1611 (2015). https://doi.org/10.1002/mds.26431

23 Dominguez Conde, C. *et al.* Cross-tissue immune cell analysis reveals tissue-specific features in humans. *Science* **376**, eabl5197 (2022). https://doi.org/10.1126/science.abl5197

24 Hafler, D. A. *et al.* In vivo activated T lymphocytes in the peripheral blood and cerebrospinal fluid of patients with multiple sclerosis. *N Engl J Med* **312**, 1405-1411 (1985). https://doi.org/10.1056/NEJM198505303122201

25 Buttner, M., Ostner, J., Muller, C. L., Theis, F. J. & Schubert, B. scCODA is a Bayesian model for compositional single-cell data analysis. *Nat Commun* **12**, 6876 (2021). https://doi.org/10.1038/s41467-021-27150-6

26 Siderowf, A. *et al.* Assessment of heterogeneity among participants in the Parkinson's Progression Markers Initiative cohort using alpha-synuclein seed amplification: a cross-sectional study. *Lancet Neurol* **22**, 407-417 (2023). https://doi.org/10.1016/S1474-4422(23)00109-6

27 Kouli, A. *et al.* T lymphocyte senescence is attenuated in Parkinson's disease. *J Neuroinflammation* **18**, 228 (2021). https://doi.org/10.1186/s12974-021-02287-9

28 Harroud, A. & Hafler, D. A. Common genetic factors among autoimmune diseases. *Science* **380**, 485-490 (2023). https://doi.org/10.1126/science.adg2992

29 Lincoln, M. R. *et al.* Genetic mapping across autoimmune diseases reveals shared associations and mechanisms. *Nat Genet* **56**, 838-845 (2024). https://doi.org/10.1038/s41588-024-01732-8

30 TNF neutralization in MS: results of a randomized, placebo-controlled multicenter study. The Lenercept Multiple Sclerosis Study Group and The University of British Columbia MS/MRI Analysis Group. *Neurology* **53**, 457-465 (1999).

31 Sicotte, N. L. & Voskuhl, R. R. Onset of multiple sclerosis associated with anti-TNF therapy. *Neurology* **57**, 1885-1888 (2001). https://doi.org/10.1212/wnl.57.10.1885

32 Wei, J. *et al.* Systems Analysis of Immune Changes after B-cell Depletion in Autoimmune Multiple Sclerosis. *bioRxiv* (2024). https://doi.org/10.1101/2024.02.07.576204

33 Yasumizu, Y. *et al.* Single-cell transcriptome landscape of circulating CD4(+) T cell populations in autoimmune diseases. *Cell Genom* **4**, 100473 (2024). https://doi.org/10.1016/j.xgen.2023.100473

34 Yasumizu, Y. PBMC/CSF single-cell RNAseq CD4+ T cell reference mapping. *protocol.io* (2025). https://doi.org/dx.doi.org/10.17504/protocols.io.q26g7mqj1gwz/v1

35 Zhang, L. *et al.* Lineage tracking reveals dynamic relationships of T cells in colorectal cancer. *Nature* **564**, 268-272 (2018). https://doi.org/10.1038/s41586-018-0694-x

36 Olah, M. *et al.* Single cell RNA sequencing of human microglia uncovers a subset associated with Alzheimer's disease. *Nat Commun* **11**, 6129 (2020). https://doi.org/10.1038/s41467-020-19737-2

37 N, M. P. *et al.* A multi-region single nucleus transcriptomic atlas of Parkinson's disease. *Sci Data* **11**, 1274 (2024). https://doi.org/10.1038/s41597-024-04117-y

38 Longhena, F. *et al.* Alpha-synuclein aggregation and dopaminergic neuron death in a new mouse model of Parkinson’s disease expressing human full-length and C-terminally

truncated 1- 120 alpha-synuclein. *bioRxiv*, 2025.2004.2013.647581 (2025). https://doi.org/10.1101/2025.04.13.647581

39 Efremova, M., Vento-Tormo, M., Teichmann, S. A. & Vento-Tormo, R. CellPhoneDB: inferring cell-cell communication from combined expression of multi-subunit ligand-receptor complexes. *Nat Protoc* **15**, 1484-1506 (2020). https://doi.org/10.1038/s41596-020-0292-x

40 Schonhoff, A. M. *et al.* Border-associated macrophages mediate the neuroinflammatory response in an alpha-synuclein model of Parkinson disease. *Nat Commun* **14**, 3754 (2023). https://doi.org/10.1038/s41467-023-39060-w

41 Kimura, K. *et al.* Immune checkpoint TIM-3 regulates microglia and Alzheimer's disease. *Nature* (2025). https://doi.org/10.1038/s41586-025-08852-z

42 Zhang, M. J. *et al.* Polygenic enrichment distinguishes disease associations of individual cells in single-cell RNA-seq data. *Nat Genet* **54**, 1572-1580 (2022). https://doi.org/10.1038/s41588-022-01167-z

43 Krohn, L. *et al.* Genome-wide association study of REM sleep behavior disorder identifies polygenic risk and brain expression effects. *Nat Commun* **13**, 7496 (2022). https://doi.org/10.1038/s41467-022-34732-5

44 Chia, R. *et al.* Genome sequencing analysis identifies new loci associated with Lewy body dementia and provides insights into its genetic architecture. *Nat Genet* **53**, 294-303 (2021). https://doi.org/10.1038/s41588-021-00785-3

45 Galiano-Landeira, J., Torra, A., Vila, M. & Bove, J. CD8 T cell nigral infiltration precedes synucleinopathy in early stages of Parkinson's disease. *Brain* **143**, 3717-3733 (2020). https://doi.org/10.1093/brain/awaa269

46 Qin, H. *et al.* Inhibition of the JAK/STAT Pathway Protects Against alpha-Synuclein-Induced Neuroinflammation and Dopaminergic Neurodegeneration. *J Neurosci* **36**, 5144-5159 (2016). https://doi.org/10.1523/JNEUROSCI.4658-15.2016

47 Lashgari, N. A. *et al.* The involvement of JAK/STAT signaling pathway in the treatment of Parkinson's disease. *J Neuroimmunol* **361**, 577758 (2021). https://doi.org/10.1016/j.jneuroim.2021.577758

48 Yan, Z., Gibson, S. A., Buckley, J. A., Qin, H. & Benveniste, E. N. Role of the JAK/STAT signaling pathway in regulation of innate immunity in neuroinflammatory diseases. *Clin Immunol* **189**, 4-13 (2018). https://doi.org/10.1016/j.clim.2016.09.014

49 Fauny, M. *et al.* Paradoxical gastrointestinal effects of interleukin-17 blockers. *Ann Rheum Dis* **79**, 1132-1138 (2020). https://doi.org/10.1136/annrheumdis-2020-217927

50 Kim, S. *et al.* Transneuronal Propagation of Pathologic alpha-Synuclein from the Gut to the Brain Models Parkinson's Disease. *Neuron* **103**, 627-641 e627 (2019). https://doi.org/10.1016/j.neuron.2019.05.035

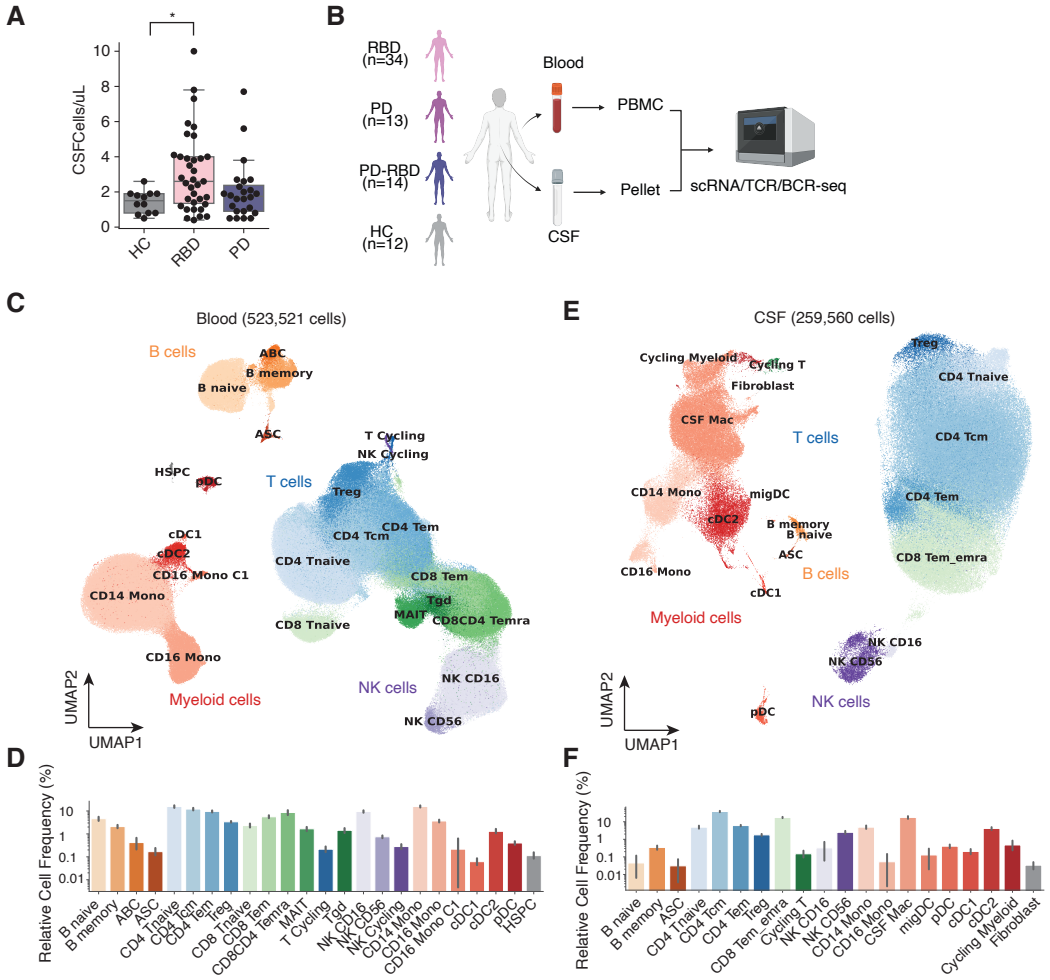
A
CSFCells/uL
HC
RBD
PD
B
RBD (n=34)
PD (n=13)
PD-RBD (n=14)
HC (n=12)
Blood
CSF
PBMC
Pellet
scRNA/TCR/BCR-seq
C
Blood (523,521 cells)
B cells
T cells
Myeloid cells
NK cells
UMAP1
UMAP2
E
CSF (259,560 cells)
T cells
B cells
Myeloid cells
NK cells
D
Relative Cell Frequency (%)
F
Relative Cell Frequency (%)

Figure 1

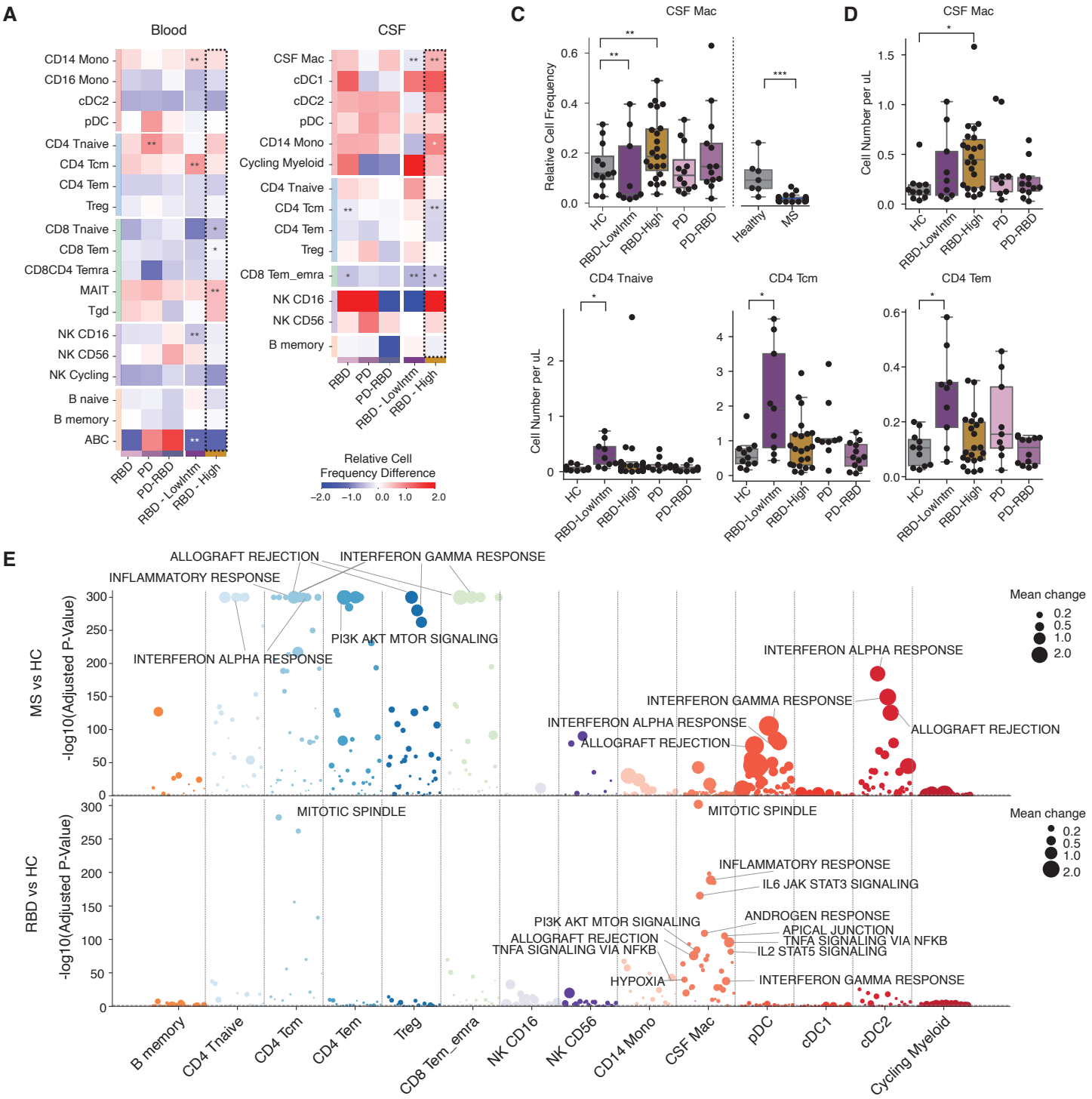
A
Blood
CSF
CD14 Mono
CD16 Mono
cDC2
pDC
CD4 Tnaive
CD4 Tcm
CD4 Tem
Treg
CD8 Tnaive
CD8 Tem
CD8CD4 Temra
MAIT
Tgd
NK CD16
NK CD56
NK Cycling
B naive
B memory
ABC
CSF Mac
cDC1
CD14 Mono
Cycling Myeloid
CD8 Tem_emra
RBD
PD
PD-RBD
RBD - LowIntm
RBD - High
Relative Cell Frequency Difference
−2.0 −1.0 0.0 1.0 2.0
C
CSF Mac
Relative Cell Frequency
HC
RBD-LowIntm
RBD-High
PD
PD-RBD
Healthy
MS
D
CSF Mac
Cell Number per uL
CD4 Tnaive
CD4 Tcm
CD4 Tem
E
ALLOGRAFT REJECTION
INTERFERON GAMMA RESPONSE
INFLAMMATORY RESPONSE
PI3K AKT MTOR SIGNALING
INTERFERON ALPHA RESPONSE
MS vs HC
-log10(Adjusted P-Value)
Mean change
0.2
0.5
1.0
2.0
MITOTIC SPINDLE
IL6 JAK STAT3 SIGNALING
ANDROGEN RESPONSE
APICAL JUNCTION
TNFA SIGNALING VIA NFKB
IL2 STAT5 SIGNALING
HYPOXIA
RBD vs HC
B memory
CD4 Tnaive
CD4 Tcm
CD4 Tem
Treg
CD8 Tem_emra
NK CD16
NK CD56
CD14 Mono
CSF Mac
pDC
cDC1
cDC2
Cycling Myeloid

Figure 2

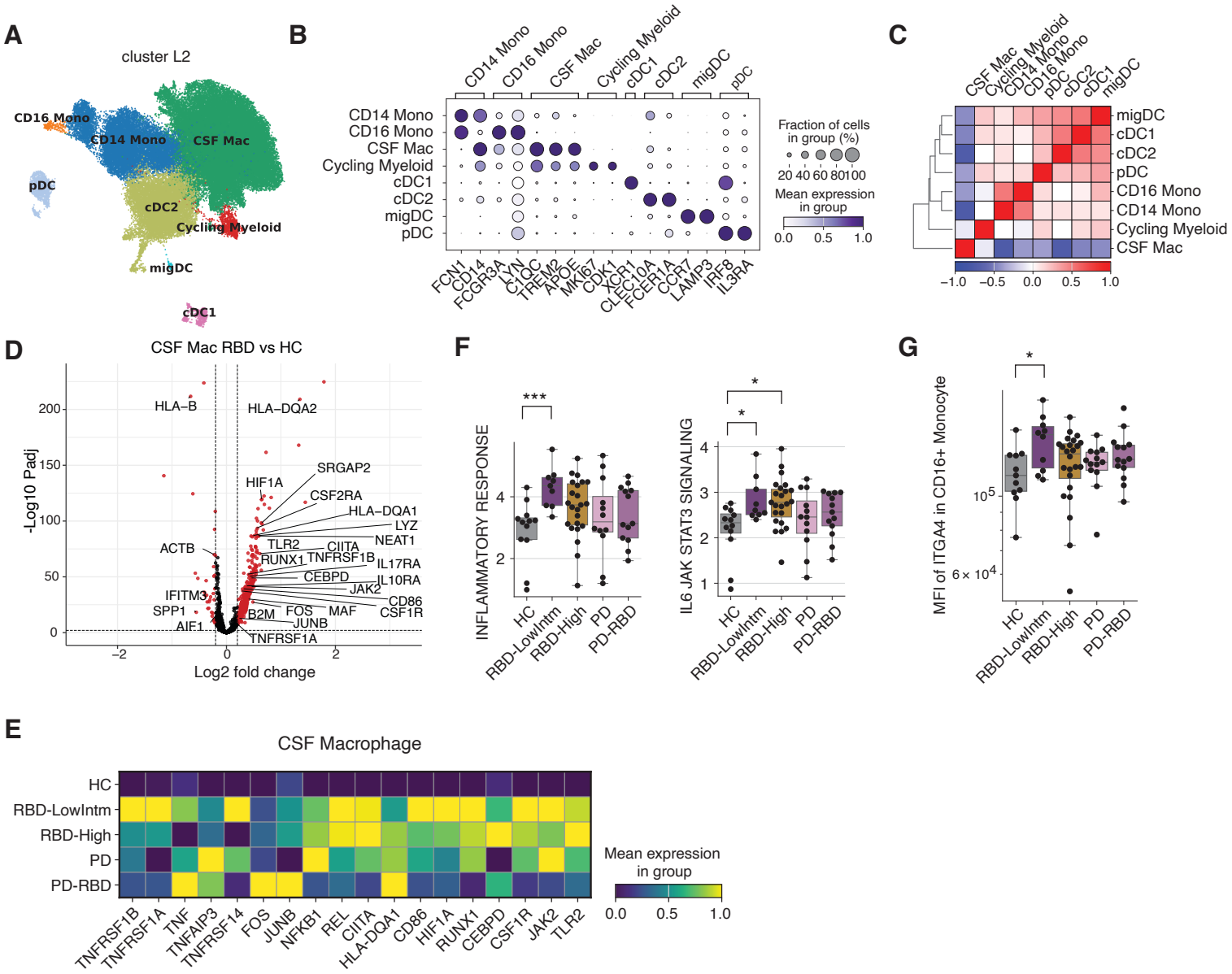
A
cluster L2
CD16 Mono
CD14 Mono
CSF Mac
pDC
cDC2
Cycling Myeloid
migDC
cDC1
B
CD14 Mono
CD16 Mono
CSF Mac
Cycling Myeloid
cDC1
cDC2
migDC
pDC
FCN1
CD14
FCGR3A
LYN
C1QC
TREM2
APOE
MKI67
CDK1
XCR1
CLEC10A
FCER1A
CCR7
LAMP3
IRF8
IL3RA
Fraction of cells in group (%)
20 40 60 80 100
Mean expression in group
0.0 0.5 1.0
C
CSF Mac
Cycling Myeloid
CD14 Mono
CD16 Mono
pDC
cDC2
cDC1
migDC
−1.0 −0.5 0.0 0.5 1.0
D
CSF Mac RBD vs HC
-Log10 Padj
Log2 fold change
HLA–B
HLA–DQA2
SRGAP2
HIF1A
CSF2RA
HLA–DQA1
LYZ
NEAT1
ACTB
TLR2
CIITA
RUNX1
TNFRSF1B
IL17RA
CEBPD
IL10RA
JAK2
IFITM3
CD86
SPP1
B2M
FOS
MAF
CSF1R
AIF1
JUNB
TNFRSF1A
F
INFLAMMATORY RESPONSE
IL6 JAK STAT3 SIGNALING
HC
RBD-LowIntm
RBD-High
PD
PD-RBD
G
MFI of ITGA4 in CD16+ Monocyte
E
CSF Macrophage
HC
RBD-LowIntm
RBD-High
PD
PD-RBD
TNFRSF1B
TNFRSF1A
TNF
TNFAIP3
TNFRSF14
FOS
JUNB
NFKB1
REL
CIITA
HLA-DQA1
CD86
HIF1A
RUNX1
CEBPD
CSF1R
JAK2
TLR2
Mean expression in group
0.0 0.5 1.0

Figure 3

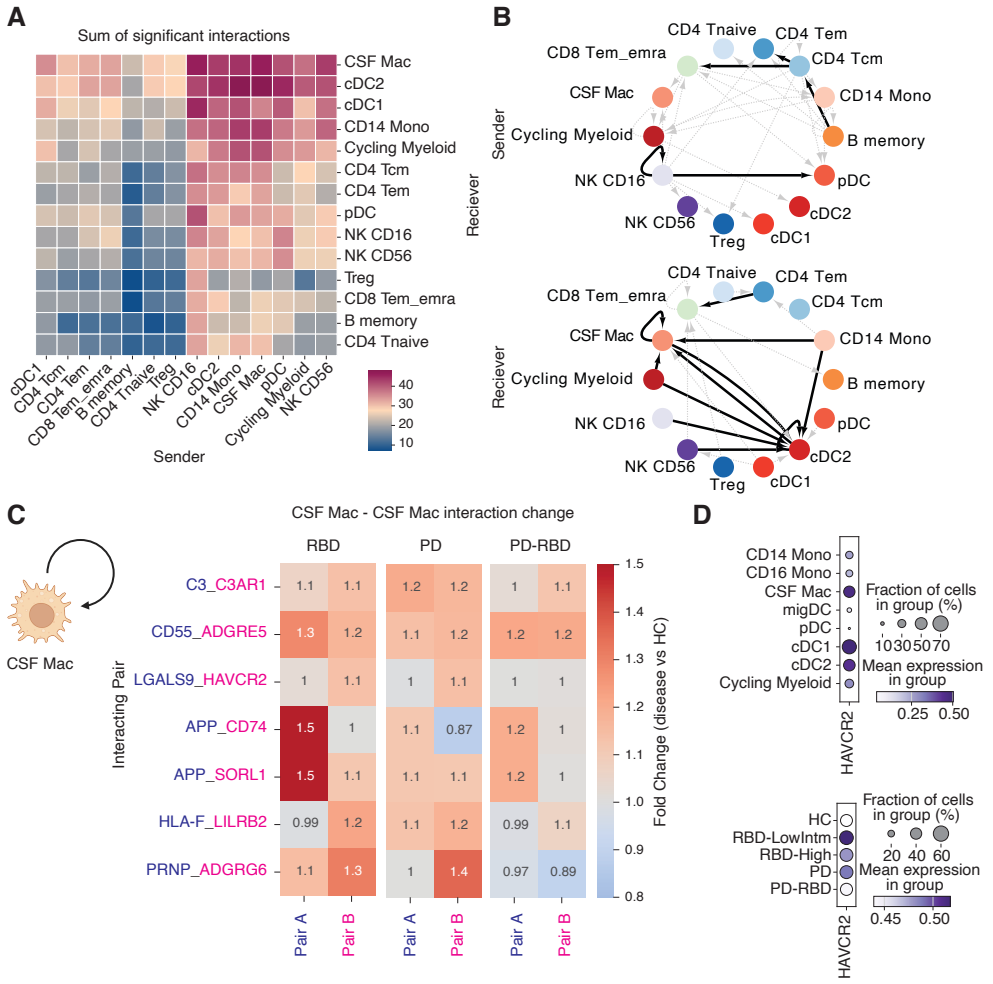
A
Sum of significant interactions
CSF Mac
cDC2
cDC1
CD14 Mono
Cycling Myeloid
CD4 Tcm
CD4 Tem
pDC
NK CD16
NK CD56
Treg
CD8 Tem_emra
B memory
CD4 Tnaive
Sender
40
30
20
10
B
Sender
Reciever
CD4 Tnaive
CD4 Tem
CD8 Tem_emra
CD4 Tcm
CSF Mac
CD14 Mono
Cycling Myeloid
B memory
NK CD16
pDC
NK CD56
cDC2
Treg
cDC1
C
CSF Mac
CSF Mac - CSF Mac interaction change
RBD
PD
PD-RBD
Interacting Pair
C3_C3AR1
CD55_ADGRE5
LGALS9_HAVCR2
APP_CD74
APP_SORL1
HLA-F_LILRB2
PRNP_ADGRG6
Pair A
Pair B
Fold Change (disease vs HC)
D
CD14 Mono
CD16 Mono
CSF Mac
migDC
pDC
cDC1
cDC2
Cycling Myeloid
HAVCR2
Fraction of cells in group (%)
Mean expression in group
HC
RBD-LowIntm
RBD-High
PD
PD-RBD

Figure 4

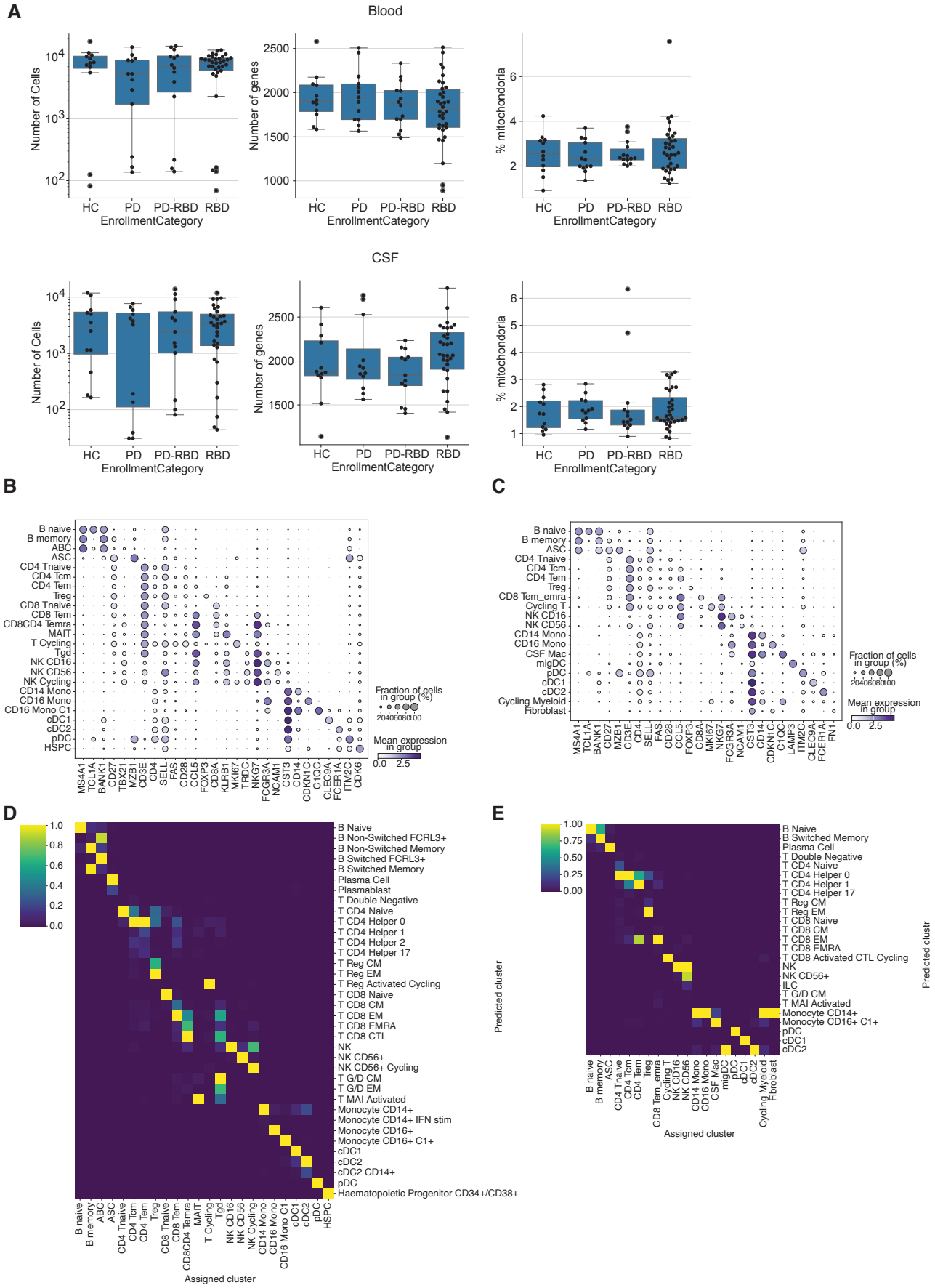

Supplementary Figure 1

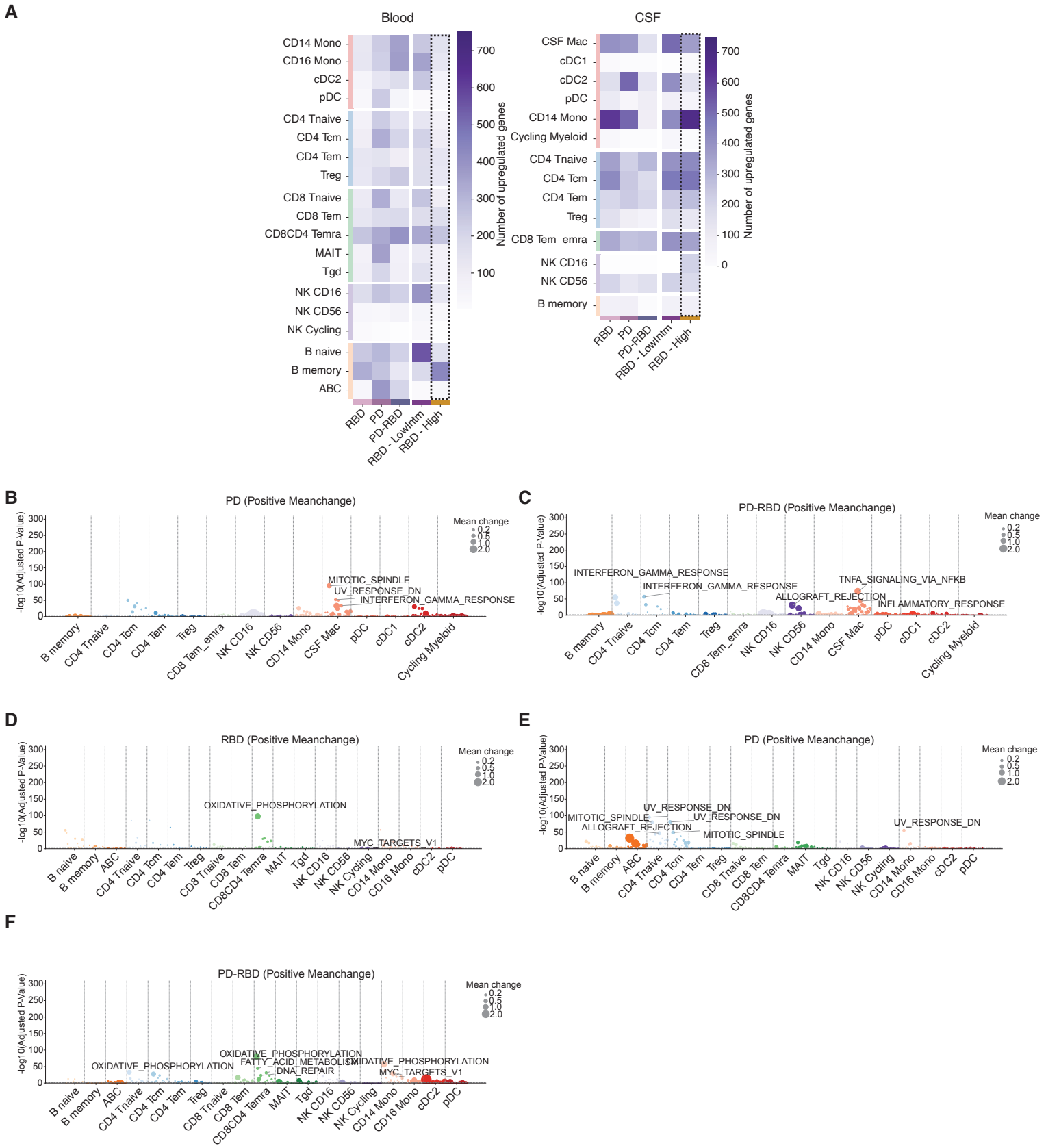

Supplementary Figure 2

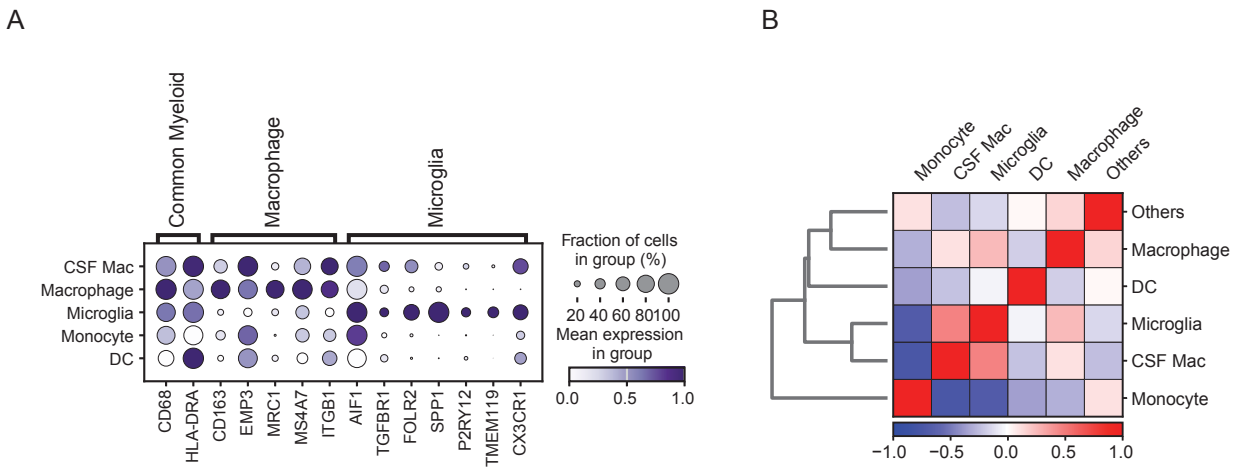

Supplementary Figure 3

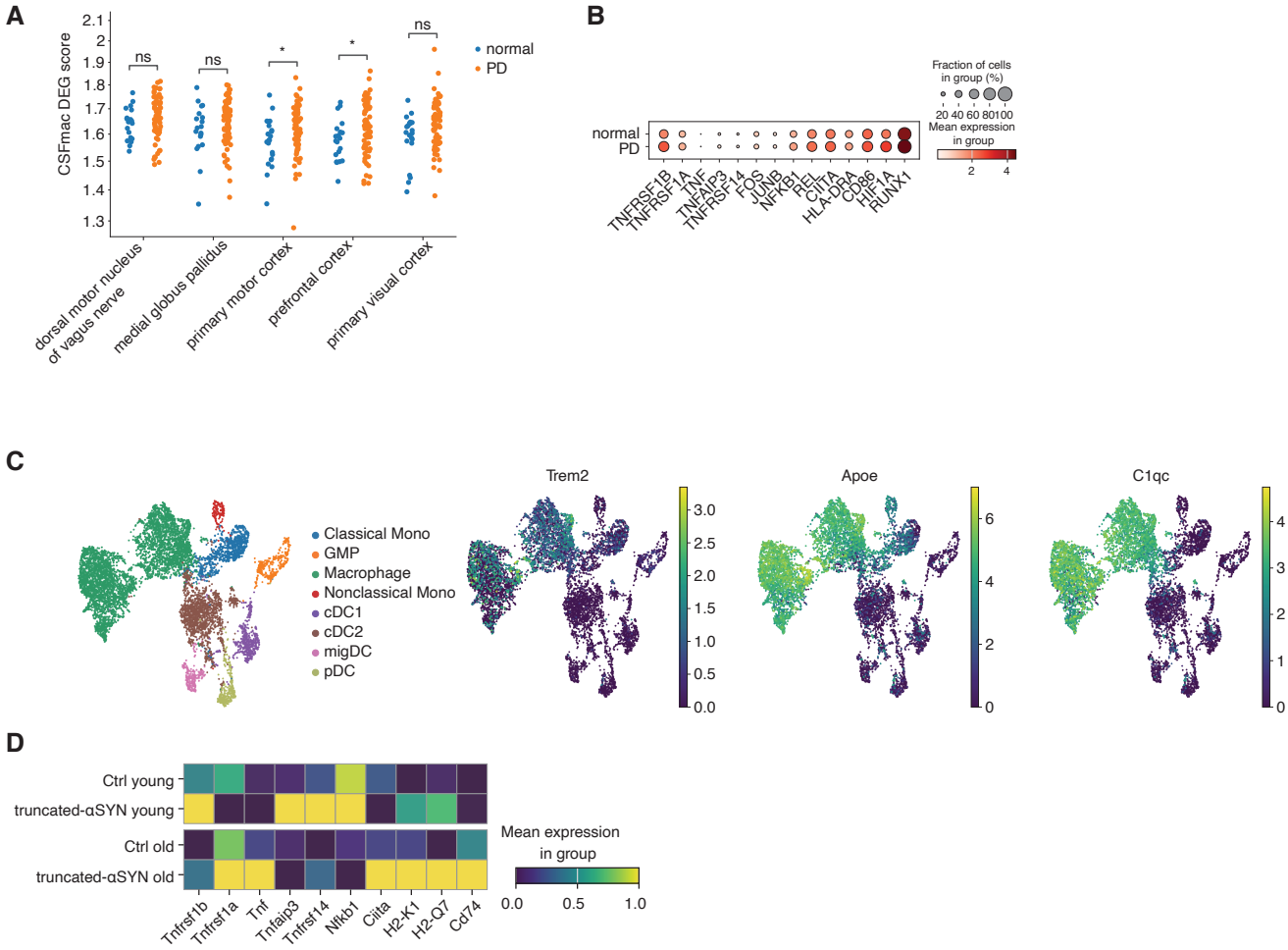

Supplementary Figure 4

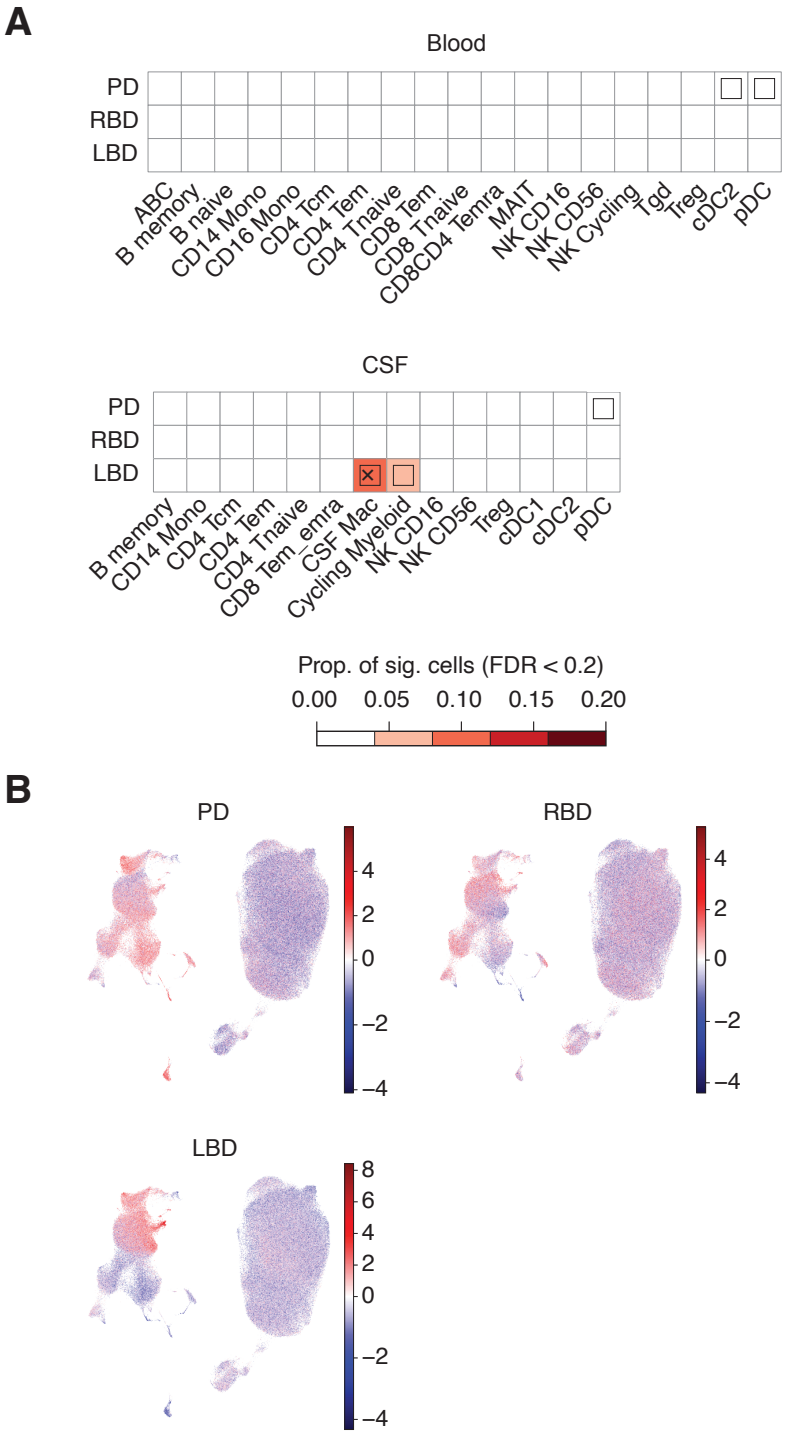

Supplementary Figure 5

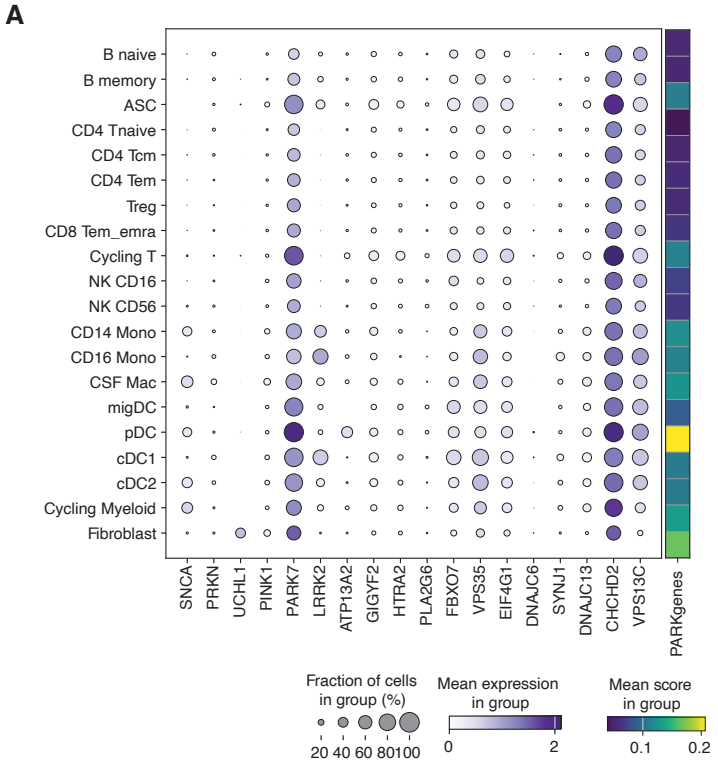

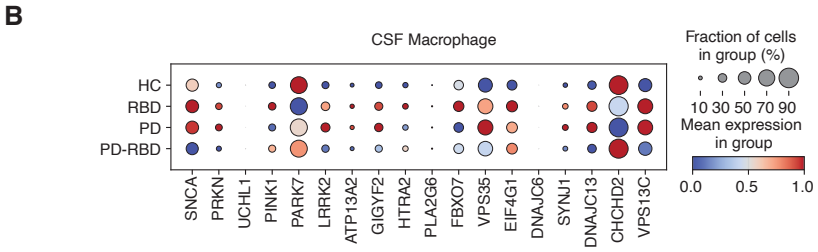

Supplementary Figure 6

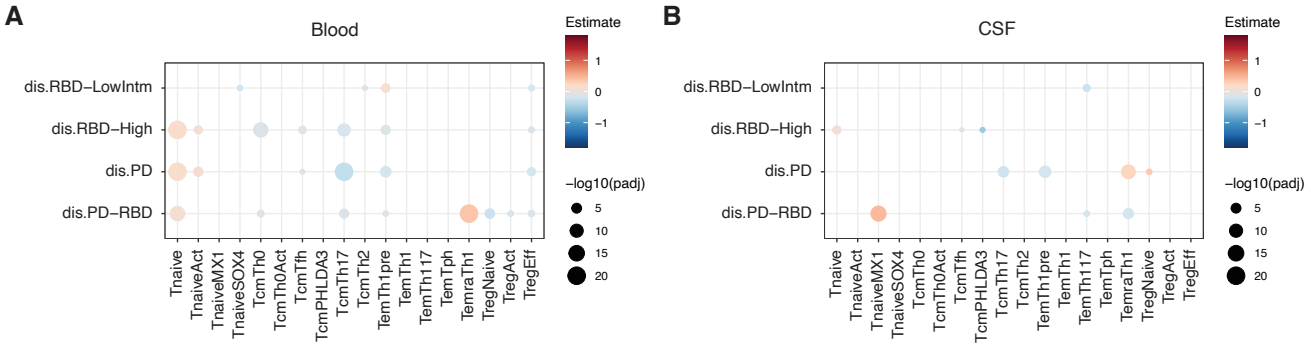

Supplementary Figure 7

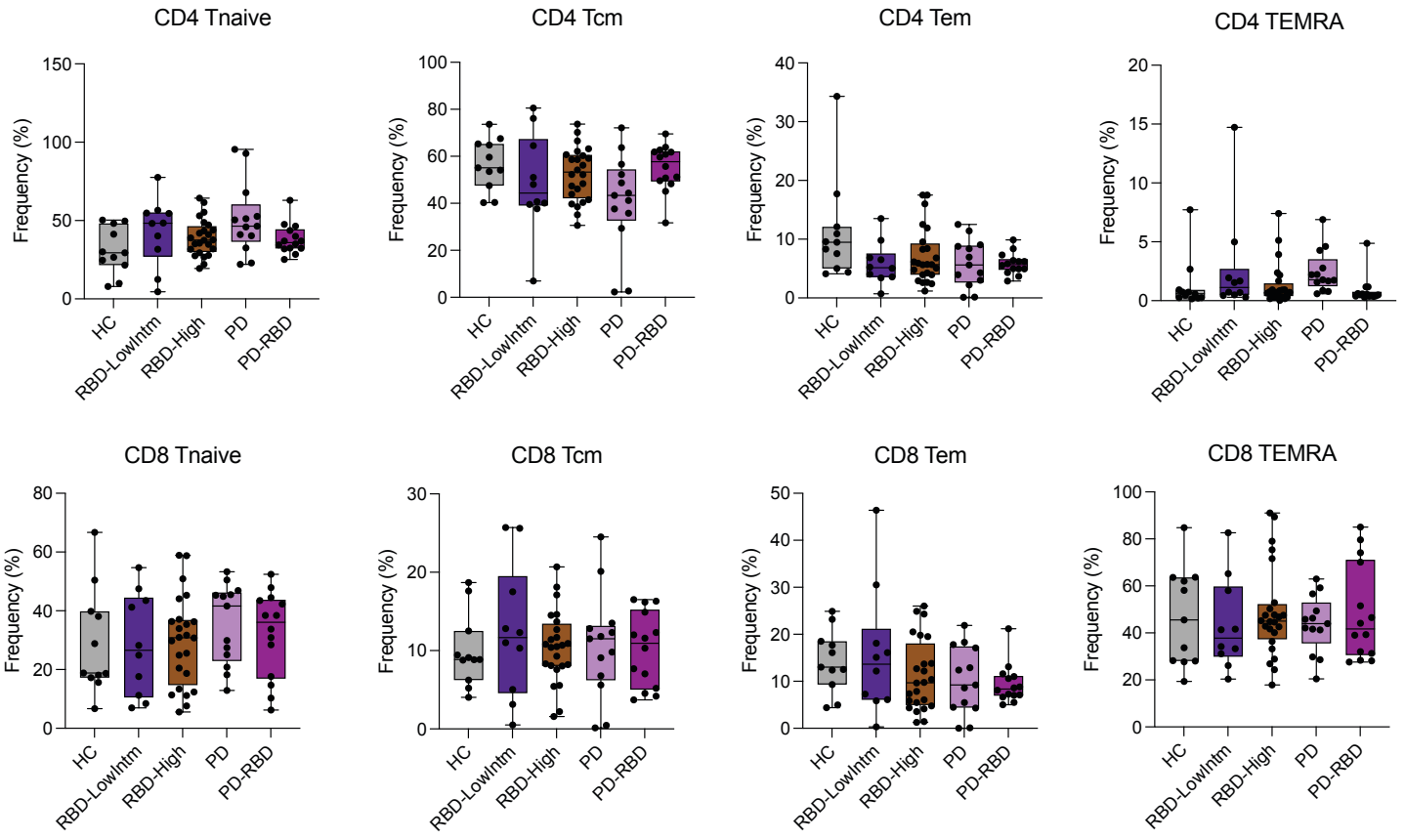

Supplementary Figure 8

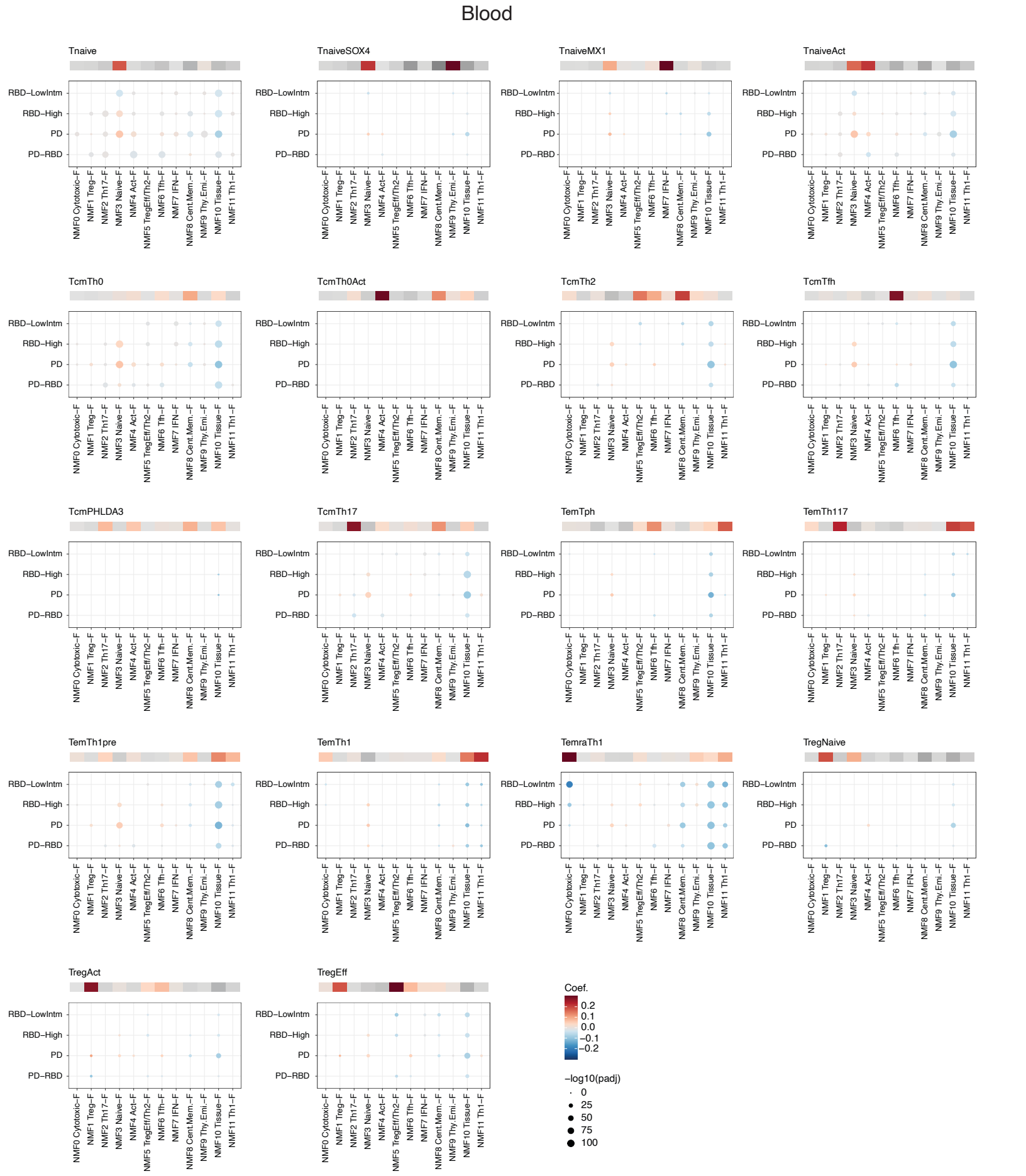

Supplementary Figure 9

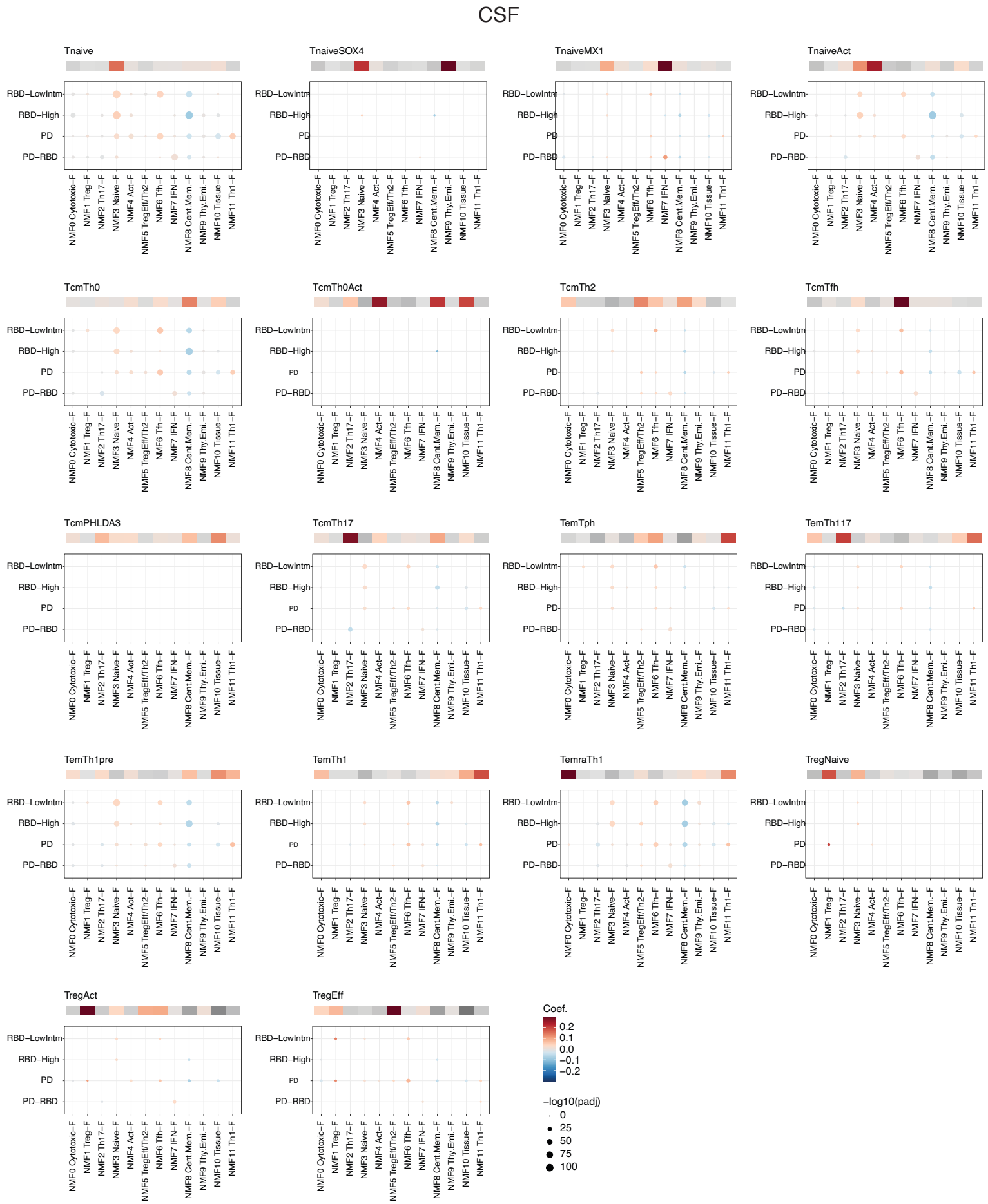

Supplementary Figure 10

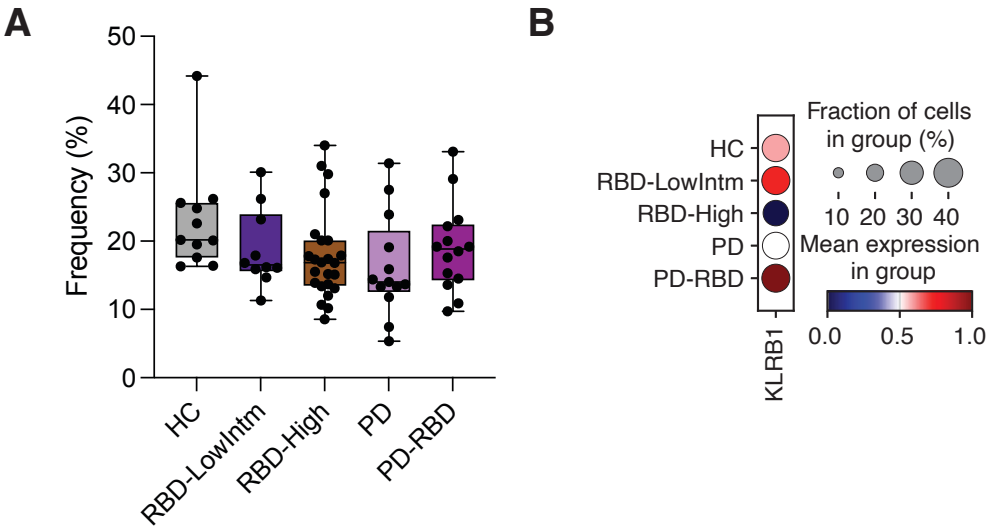

Supplementary Figure 11

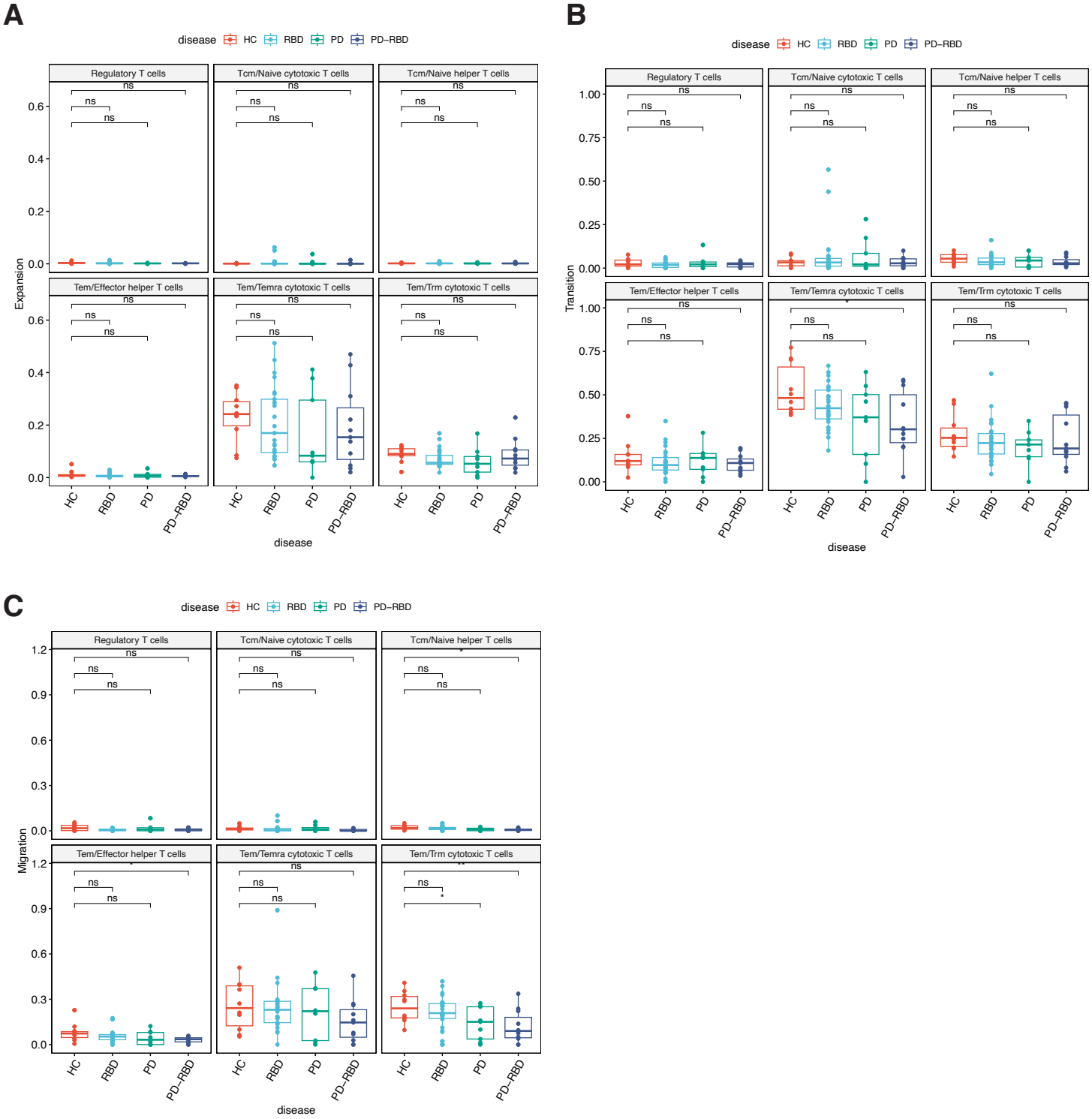

Supplementary Figure 12

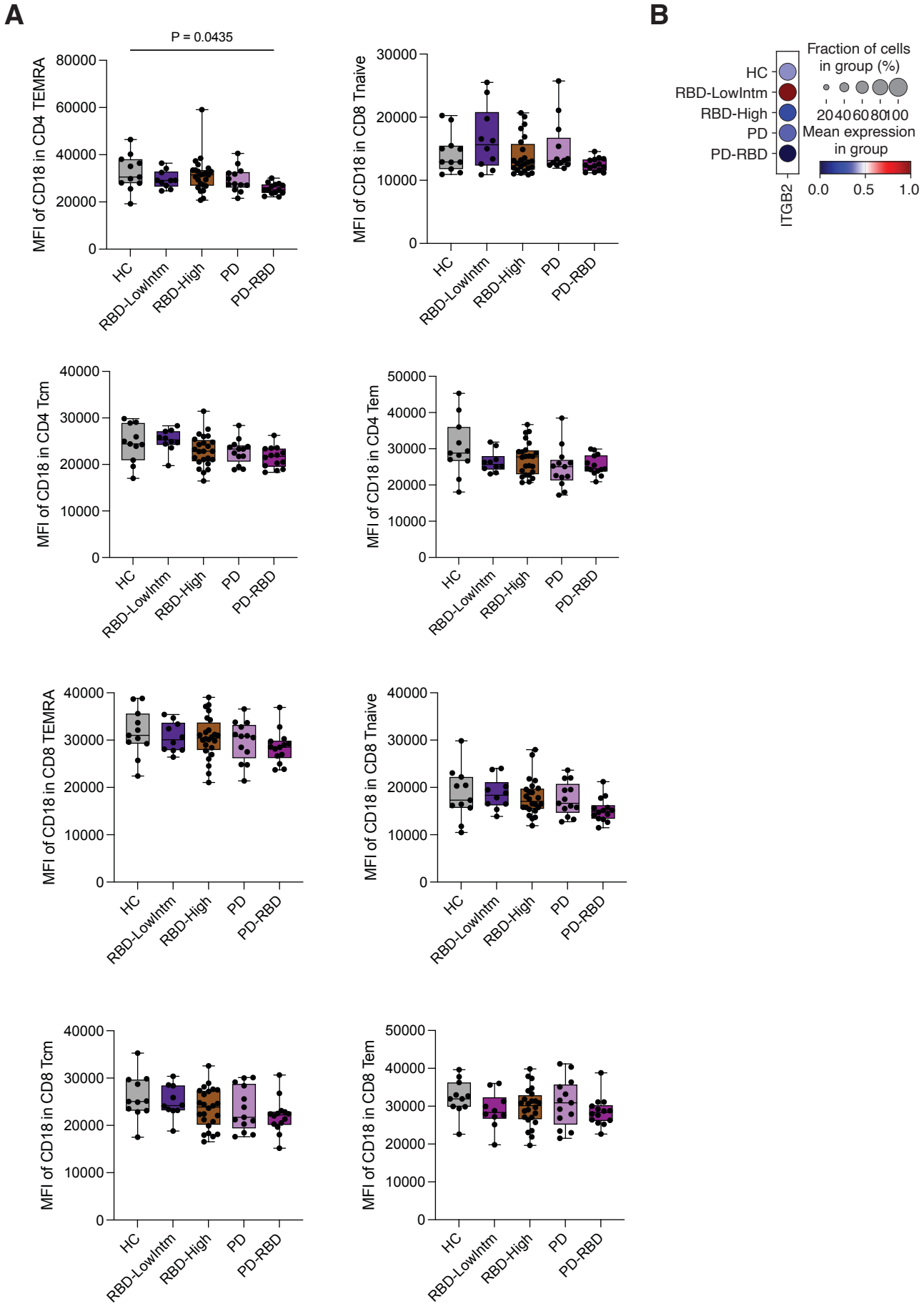

Supplementary Figure 13